DALTON
FULL PAPER

Metal-to-ligand charge-transfer excited-states in binuclear copper(I) complexes. Tuning MLCT excited-states through structural modification of bridging ligands. A resonance Raman study

Mark R. Waterland,† Amar Flood and Keith C. Gordon *

Department of Chemistry, University of Otago, PO Box 56, Dunedin, New Zealand. E-mail: kgordon@alkali.otago.ac.nz

Received 12th July 1999, Accepted 18th November 1999

The resonance Raman spectra of the ground- and lowest excited-states for a series of binuclear copper(I) complexes with bridging ligands based on 2,3-di-(2-pyridyl)quinoxaline have been measured. Analyses of the ground-state resonance Raman spectra show strong enhancement of an inter-ring stretching mode and quinoxaline-based modes; consistent with the Frank–Condon state having bonding changes about the copper(I) centre and on the quinoxaline ring system. The electronic absorption data also suggest the initially formed MLCT-state is localised towards the quinoxaline ring system. The excited-state resonance Raman spectroscopy shows similar spectral features for complexes which have substituent changes at the pyridyl rings of the bridging ligand. They show spectra associated with the radical anion of the bridging ligand. This is consistent with the formation of an excited-state which is metal-to-ligand charge-transfer in nature and where the radical anion is localised on the quinoxaline ring system of the bridging ligand.

Introduction

The metal-to-ligand charge-transfer (MLCT) states of transition metal complexes with polypyridyl ligands show considerable promise as charge-transfer sensitisers in solar energy conversion schemes.[1] Incorporating a ligand with two chelation sites into the coordination sphere allows systematic construction of large supramolecular assemblies, capable of acting as antennae in these energy conversion schemes.[2] A rational study of the properties of these large multi-nuclear assemblies begins with an investigation of the smaller units such as mono- and binuclear complexes. This study investigates the lowest MLCT-state of some binuclear copper(I) systems that incorporate the bridging ligand 2,3-di(2-pyridyl)quinoxaline (dpq) and some of its simple derivatives. The complexes have interesting properties; firstly, the copper(I) centre provides a unique mechanism for controlling the photophysics in the excited-state. In the MLCT-state the copper(I) centre is formally oxidised to the copper(II) oxidation state. In coordinating solvents (*e.g.* methanol) this MLCT-state is rapidly quenched by exciplex formation with the copper(II) centre.[3] Methyl groups can be used to block the approach of the solvent quencher molecule and thus extend the MLCT excited-state lifetime. Hence, a series of ligands with a methyl group at the 6′-position of the pyridyl ring have been utilised in this study (Fig. 1). Secondly, the addition of methyl and other groups alters the electronic energy of the π-accepting properties of the bridging ligand. In these binuclear systems the energy of the π-acceptor MO is an important factor in controlling the extent of metal–metal communication.[4] The addition of electron-withdrawing and -donating moieties provides a means for fine-tuning this degree of communication.

The aims of this study were two-fold. Firstly, to establish the nature of the Frank–Condon (FC) state into which the excited electron is transferred upon MLCT excitation and how this is altered by substituents at the pyridyl and quinoxaline ring systems. Secondly, to characterise the excited-state created after relaxation from the FC-state.

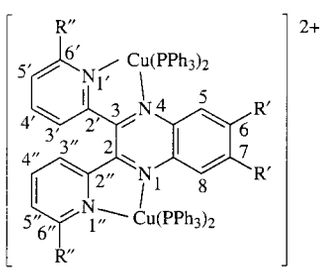

Fig. 1 Ligands and numbering scheme: R″ = R′ = H, **1**; R″ = H, R′ = benzo, **2**; R″ = H, R′ = CH_3 **3**; R″ = H, R′ = Cl, **4**; R″ = CH_3, R′ = H, **5**; R″ = CH_3, R′ = benzo, **6**; R″ = CH_3, R′ = CH_3, **7**; R″ = CH_3, R′ = Cl, **8**.

This paper presents the resonance Raman spectra of a series of binuclear copper(I) systems containing the dpq ligand. The effects of substitutions at the pyridyl and quinoxaline rings of the bridging ligands will be discussed. Resonance Raman spectroscopy provides a detailed probe of the nuclear geometry changes that occur in the FC region immediately following photoexcitation. Broad unstructured absorption bands, that are typical of MLCT transitions, are indicative of systems that undergo so-called 'short-time' dynamics[5] on the excited-state surface. When only a single electronic excited-state contributes to the scattering tensor, the resonance Raman intensities may be simply related to excited-state geometry displacements in the 'short-time' regime.[6] Modes that are able to mimic the nuclear geometry changes that occur upon electronic excitation will be selectively enhanced when the frequency of the laser radiation field approaches resonance with the electronic transition.[7,8] The relative intensities of the observed bands may be related to the normal coordinate displacement (Δ) on going from the ground- to excited-state.

Resonance Raman scattering, in the condensed phase, is physically a short-time effect ($\approx 10^{-15}$ s) and as such provides information for only the FC region on the excited-state surface. Pulsed excitation may be used to create a significant excited-

† Present address: Department of Chemistry, Kansas State University, Manhattan, Kansas, USA.

This journal is © The Royal Society of Chemistry 2000

state population that can generate Raman scattering and thus serve as a probe for the populated excited-state. For the pulse duration (approx. 10 ns) that we employ, the majority of the scattering from the excited-state comes from the thermally-equilibrated excited (THEXI)[9] state. In this paper we also present time-resolved resonance Raman (TR^3) spectra and compare structural changes evident in the FC region with the geometry in the THEXI-state.

Experimental

Synthesis

The ligands were synthesised by literature methods.[10] In a typical procedure, one equivalent of the appropriately substituted 1,2-diaminobenzene (2.1 mmol) was added to a solution of 500 mg (2.1 mmol) of 2,2′-(6-methylpyridyl) in ethanol (100 mL) and refluxed for 12 h in the absence of light. The volume was reduced and sufficient water added to initialise precipitation. The solution was then heated until dissolution occurred. The product that separated upon cooling was isolated by vacuum filtration and washed several times with an ice-cold water–ethanol mixture (50 : 50 v : v) and recrystallised from a water–ethanol mixture of the same composition.

Binuclear copper(I) complexes of each ligand were prepared from the copper(I) precursor, bis(acetonitrile)bis(triphenylphosphine)copper(I) tetrafluoroborate $[Cu(PPh_3)_2(MeCN)_2]\cdot[BF_4]$ and the appropriate ligand, following the method of Yam and Lo.[11] One equivalent of bridging ligand (50 mg, 0.17 mmol) was added to a stirred, degassed solution of dichloromethane (20 mL) containing 2 mol equivalents (266 mg, 0.34 mmol) of $[Cu(PPh_3)_2(MeCN)_2]\cdot[BF_4]$ under an argon atmosphere. A deep red colour formed immediately. The solution was stirred for a further 10 min then evaporated to dryness. The complex was dissolved into 3 mL of dichloromethane and crystallised *via* diethyl ether diffusion. The purity of the complexes $[(PPh_3)_2Cu(dpq)Cu(PPh_3)_2]\cdot[BF_4]_2$, **1**·$(BF_4)_2$, [dpq = 2,3-di(2-pyridyl)quinoxaline], $[(PPh_3)_2Cu(dpb)Cu(PPh_3)_2]\cdot[BF_4]_2$, **2**·$(BF_4)_2$, {dpb = 2,3-di(2-pyridyl)benzo[*g*]quinoxaline}, $[(PPh_3)_2Cu(dpqMe_2)Cu(PPh_3)_2]\cdot[BF_4]_2$, **3**·$(BF_4)_2$, [dpq$Me_2$ = 6,7-dimethyl-2,3-di(2-pyridyl)quinoxaline] and $[(PPh_3)_2Cu(dpqCl_2)Cu(PPh_3)_2]\cdot[BF_4]_2$, **4**·$(BF_4)_2$, [dpq$Cl_2$ = 6,7-dichloro-2,3-di(2-pyridyl)quinoxaline] was determined by microanalysis.

2,3-Di(6-methyl-2-pyridyl)quinoxaline (dmpq). δ_H (200 MHz, solvent $CDCl_3$, standard $SiMe_4$) 8.20 (dd, 2H), 7.79 (dd, 2H), 7.67 (d, 4H), 7.08 (dd, 2H), 2.28 (s, 6H) (Found C, 76.78; H, 5.22; N, 17.80. Calculated C, 76.90; H, 5.16; N, 17.94%): yield = 34%.

2,3-Di(6-methyl-2-pyridyl)benzo[*g*]quinoxaline (dmpb). δ_H (200 MHz, solvent $CDCl_3$, standard $SiMe_4$) 8.79 (s, 2H), 8.13 (dd, 2H), 7.82 (d, 2H), 7.71 (t, 2H), 7.59 (dd, 2H), 7.10 (d, 2H), 2.27 (s, 6H) (Found C, 79.36; H, 5.23; N, 15.36. Calculated C, 79.53; H, 5.01; N, 15.46%): yield = 40%.

6,7-Dimethyl-2,3-di(6-methyl-2-pyridyl)quinoxaline (dmpqMe_2). δ_H (200 MHz, solvent $CDCl_3$, standard $SiMe_4$) 7.96 (s, 2H), 7.65 (t, 4H), 7.08 (dd, 2H), 2.53 (s, 6H), 2.29 (s, 6H) (Found C, 77.50; H, 5.75; N, 16.55. Calculated C, 77.62; H, 5.92; N, 16.46%): yield = 29%.

6,7-Dichloro-2,3-di(6-methyl-2-pyridyl)quinoxaline (dmpqCl_2). δ_H (200 MHz, solvent $CDCl_3$, standard $SiMe_4$) 8.34 (s, 2H), 7.71 (t, 4H), 7.12 (dd, 2H), 2.27 (s, 6H) (Found C, 62.92; H, 3.47; N, 14.68. Calculated C, 63.01; H, 3.70; N, 14.70%): yield = 18%.

$[(PPh_3)_2Cu(dmpq)Cu(PPh_3)_2]\cdot[BF_4]_2$ (5·$[BF_4]_2$·0.5CH_2Cl_2). (Found C, 65.60; H, 4.66; N, 3.39; F, 8.40. Calculated C, 65.20; H, 4.55; N, 3.28; F, 8.91%): yield = 70%.

$[(PPh_3)_2Cu(dmpb)Cu(PPh_3)_2]\cdot[BF_4]_2$ (6·$[BF_4]_2$·1.5CH_2Cl_2). (Found C, 63.34; H, 4.65; N, 3.05; F, 7.53. Calculated C, 63.66; H, 4.55; N, 3.05; F, 8.25%): yield = 85%.

$[(PPh_3)_2Cu(dmpqMe_2)Cu(PPh_3)_2]\cdot[BF_4]_2$ (7·$[BF_4]_2$·0.5CH_2Cl_2). (Found C, 65.84; H, 4.86; N, 3.21; F, 8.41. Calculated C, 65.50; H, 4.71; N, 3.23; F, 8.76%): yield = 81%.

$[(PPh_3)_2Cu(dmpqCl_2)Cu(PPh_3)_2]\cdot[BF_4]_2$ (8·$[BF_4]_2$·0.5CH_2Cl_2). (Found C, 62.45; H, 4.39; N, 3.21; F, 7.90. Calculated C, 62.64; H, 4.26; N, 3.16; F, 8.56%): yield = 79%.

Physical measurements and calculations

Either a continuous-wave Spectra-Physics Model 166 argon-ion laser or an Optlectra helium–neon laser was used to generate ground-state resonance Raman (GSRR) scattering. Band-pass filters removed the Ar^+ plasma emission lines from the laser output. Typically, the laser output was adjusted to give 25 mW at the sample. The incident beam and the collection lens were arranged in a 135° back-scattering geometry to reduce Raman intensity reduction by self-absorption.[12] An aperture-matched lens was used to focus scattered light through a narrow band line-rejection (notch) filter (Kaiser Optical Systems) and a quartz wedge (Spex) and onto the entrance slit of a spectrograph (Spex 750M). The collected light was dispersed in the horizontal plane by a 1800 grooves mm^{-1} holographic diffraction grating and detected by a liquid nitrogen-cooled 1152-EUV CCD controlled by an ST-130 controller and CSMA 2.3b(v.2) software (Princeton Instruments).

The frequency-tripled output from a Nd:YAG (Continuum Surelite I) pulsed laser (5–7 ns pulse width, operating at 10 Hz) was used to generate stimulated Raman scattering[13] for the excited state resonance Raman (ESRR) experiments. The 355 nm output from the Nd:YAG laser was focused into a 10 cm cell filled with spectrophotometric grade acetonitrile. A quartz Pellin–Broca prism was used to separate the co-linear partially depleted pump beam and four Stokes orders of stimulated Raman scattering. The second Stokes output from the Raman shifter was directed onto the sample in the same manner as the continuous-wave Raman experiments. Typically, a 355 nm, 7–30 mJ pump pulse was used, generating 0.5–2.5 mJ of the second Stokes-shifted line at 448.2 nm. The beam diameter at the sample was 300 μm.

Wavelength calibration was performed with a combination of solvent Raman lines[14] and emission lines from the argon-ion plasma. Calibrations were reproducible to within 1–2 cm^{-1}. Spectra were obtained with a resolution of 5 cm^{-1}. For resonance Raman spectra generated with λ_{ex} = 514.5, 488, 457.9 and 448.2 nm, no attempt was made to correct the Raman intensities for self-absorption or for the spectrometer response. Resonance Raman spectra generated with λ_{ex} = 632.8 nm were corrected by comparing solvent band intensities with those from the literature.[14]

Spectrophotometric grade dichloromethane (Aldrich) was used as received. Freshly prepared samples were used throughout. Sample concentrations were typically of the order of 5–10 mM. When using pulsed excitation, samples were degassed by bubbling with argon for 10 min prior to irradiation. Sample integrity following irradiation with the pulsed laser was checked by recording UV/Vis and GSRR spectra.

PM3 calculations were carried out using the PC Spartan Plus (version 1.5) software package.[15]

Results and discussion

Electronic absorption data

Electronic absorption data for the complexes are presented in Table 1. The complexes exhibit a visible absorption near 480 nm ($\varepsilon_{max} \cong 3000$ M^{-1} cm^{-1}) and a UV absorption near 370 nm

Table 1 Electronic absorption data for $[(PPh_3)_2Cu(BL)Cu(PPh_3)_2]^{2+}$ systems

Compound	$\lambda_{max}(CH_2Cl_2)$/nm ($\varepsilon \times 10^{-4}$/M^{-1} cm^{-1})
1·$(BF_4)_2$	366 (0.866), 494 (0.365)
2·$(BF_4)_2$	404 (0.754), 535 (0.257)
3·$(BF_4)_2$	372 (1.08), 488 (0.380)
4·$(BF_4)_2$	378 (1.12), 517 (0.232)
5·$(BF_4)_2$	376 (0.638), 481 (0.292)
6·$(BF_4)_2$	409 (0.691), 515 (0.362)
7·$(BF_4)_2$	379 (0.729), 464 (0.304)
8·$(BF_4)_2$	383 (0.940), 482 (0.223)

($\varepsilon_{max} \cong 10\,000$ M^{-1} cm^{-1}). The visible absorption band shifts to longer wavelength as the reduction potential of the ligand decreases[16] and is absent in the spectra of the corresponding ligand and copper precursor. On this basis this band is assigned to a MLCT transition. The possibility of a ligand-to-ligand charge-transfer (LLCT) between $PPh_3 \longrightarrow BL$ occurring in the visible region is ruled out. The related complex $[(PPh_3)_2$-Ag(phen)$]^+$, which has an LLCT transition, shows no visible absorptions.[17] In each of the complexes, a band at *ca.* 370 nm is observed. This is attributed to a $\pi \longrightarrow \pi^*$ transition of the ligand; similar absorption bands are observed for the free ligand species.

The relative energies of the absorption maxima for the complexes are consistent with the reduction potentials for these species as measured by Yam and Lo[11] and ourselves.[18] Complexes containing ligands that are more easily reduced show red-shifted MLCT absorptions. Consequently the energies of the π-accepting orbitals for the ligands follow the order $dpqMe_2 > dpq > dpb > dpqCl_2$, with a similar pattern observed for the ligands with R″ = Me, although at slightly higher energy.

Resonance Raman data

The ground state resonance Raman (GSRR) spectra show about 8–10 bands within the 1100–1650 cm^{-1} region. The data are presented in Fig. 2 and Table 2, with labels for the vibrational modes. The pattern of band enhancements and wavenumber shifts on going through the series of complexes is complicated, but a number of empirical relationships are evident. The ν_2 band is assigned as pyridyl in nature, since it lies at the appropriate wavenumber for the 8a mode of pyridine.[19] Furthermore, a study of the related dimer $[\{Ru(bpy)_2\}_2$-(μ-dpq)$]^{4+}$ (bpy = 2,2′-bipyridine) by Wertz *et al.*[20] revealed a close correspondence between the GSRR spectrum of $[\{Ru(bpy)_2\}_2(\mu\text{-dpq})]^{4+}$ and the surface-enhanced Raman scattering (SERS) spectrum of quinoxaline. The only mode that did not correlate with the SERS spectrum was at 1596 cm^{-1}, which they attributed to a pyridine-based mode. The fact that it is weakly enhanced in the reported spectra suggests the acceptor MO of the MLCT transition points away from the pyridine. The wavenumber of the ν_2 mode is increased when the pyridine ring is methyl substituted, **1** to **5** and **2** to **6**. The ν_3 mode is assigned as a delocalised vibration involving the motion of atoms on both ring systems. The wavenumber of the ν_3 mode is decreased on going to the Cl quinoxaline ring substitution and it is also shifted with methyl substitution at the pyridyl. The ν_4 mode is assigned as pyridine-based, as it is unshifted with substitution at the quinoxaline rings, *i.e.* **1** through **4**, but does shift to higher wavenumber with methyl substitution at the pyridine ring. The ν_6 mode is assigned as a quinoxaline ring stretch, decreasing in wavenumber as the electron density in the ring is reduced, **4** ⟶ **1** ⟶ **3**. The ν_9 mode is assigned as an inter-ring stretch on the basis of the wavenumber value.[18] An analysis of a series of polypyridyl and phenyl compounds[21] assigned bands in the region 1200–1350 cm^{-1} as inter-ring stretches. A detailed normal coordinate analysis of the related $[Ru(bpy)_3]^{2+}$ complex[22] also assigned a band at 1320 cm^{-1} as having inter-ring stretch character.

For **2** and **6** a number of modes are enhanced in the GSRR spectra; these lie at 1626, 1590, 1562, 1515, 1468, 1399, 1320 and 1277 cm^{-1} for **2**. The spectrum of phenazine[23] shows bands at 1556, 1479, 1403 and 1280 cm^{-1}, thus most of the bands in **2** may be assigned as phenazine-based. The residual bands at 1515 and 1320 cm^{-1} are assigned as pyridine (ν_4) and inter-ring stretches (ν_9). A number of bands (*i.e.* ν_1) are also present at high wavenumber, these are assigned as pyridyl in nature. The spectrum of **6** is very similar to that of **2** [Fig. 2(b)], with an extra band at 1395 cm^{-1}. This extra band may be due to a lowering of symmetry in the complex as a consequence of the steric crowding about the copper(I) centres, brought about by the methyl groups and the phenazine ring.

The electronic spectra for the complexes show broad structureless absorptions at about 480 and 370 nm. The pattern of band enhancements observed from the resonance Raman scattering, as a function of excitation wavelength, may provide some insight into the types of transitions present.[24] GSRR data were obtained for each of the complexes with 457.9, 488 and 514.5 nm excitation wavelengths. These span the MLCT transition present in each of the complexes. For the complexes reported herein, the GSRR spectra show the presence of 2 transitions across the excitation wavelengths used. The changes in band enhancements are exemplified by **4** (Fig. 3). This shows the enhancement of bands at 1591, 1545, 1515, 1451, 1352, 1323 and 1286 cm^{-1} with 457.9 nm excitation but only the 1545, 1451, 1352, 1323 and 1286 cm^{-1} are strongly enhanced with 514.5 nm excitation. The wavenumbers for the observed spectral bands are presented in Table 2, with an indication of their relative enhancements at differing excitation wavelengths. The general pattern of behaviour is that the higher wavenumber modes that are pyridine-based (ν_2, ν_4) are more strongly enhanced with blue excitation and the 1450–1470 (ν_6) and 1320 (ν_9) cm^{-1} bands become more enhanced with longer wavelength excitation. These enhancements patterns are consistent with the presence of two MLCT transitions which have differing acceptor π* bridging ligand MOs; that at lower energy having significant wavefunction amplitude at the quinoxaline ring, hence enhancing the quinoxaline modes, and the second having greater amplitude over the pyridyls and thereby enhancing the pyridine modes.

For the complexes with 6-methyl substituted bridging ligands, the pyridine-based modes are much less enhanced than for the corresponding nonsubstituted complexes. This is consistent with the methyl groups polarising the acceptor MO of the bridging ligand away from the pyridine groups. This polarisation of MOs has been observed previously for substituted bipyridine ligands in resonance Raman and TRIR studies.[25,26] Depolarisation ratio measurements showed the scattering to be consistent with A-term scattering (*i.e.* $\rho = 1/3$).[27] A-term scattering is also consistent with a resonance with a strongly allowed electronic transition.

In the low wavenumber region, a band is prominent at 527 cm^{-1} for **4** (Fig. 3), with weaker features close to 630 cm^{-1}. All 8 complexes show similar wavenumbers for bands in this region. Such low wavenumber vibrations are typical of out-of-plane ligand vibrations and may also contain significant metal-to-N character.[22] However, they are often not strongly enhanced because of the so-called missing mode effect.[6] Their large enhancements indicate substantial displacements from the ground-state in terms of ligand out-of-plane and metal–ligand bond length changes. This is consistent with a change in coordination number upon photoexcitation of a copper(I) complex, as discussed by McMillin and others.[3]

Attempts were made to measure the steady-state and time-resolved emission spectra for the binuclear copper systems. All systems exhibited very weak emission, the systems with R″ = Me were slightly stronger emitters than the systems with

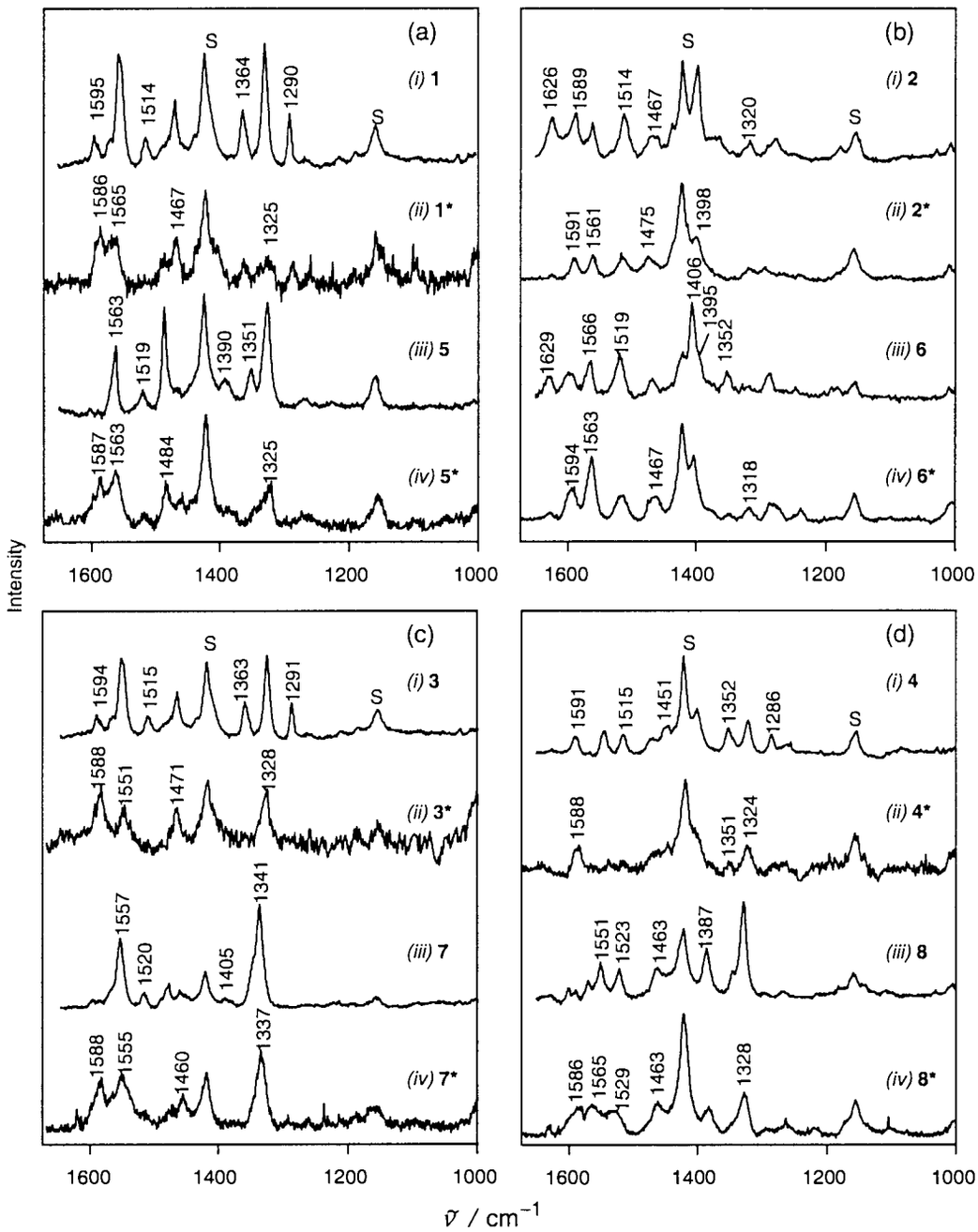

Fig. 2 Ground state resonance Raman spectra (457.9 nm continuous-wave excitation, 15 mW at sample) of 10 mM solution of complexes in CH_2Cl_2: (a)(i) **1**; (a)(iii) **5**; (b)(i) **2**; (b)(iii) **6**; (c)(i) **3**; (c)(iii) **7**; (d)(i) **4**; (d)(iii) **8**. Excited-state resonance Raman spectra (448.2 nm pulsed excitation, 2 mJ per pulse, 10 Hz) of 10 mM solutions of complexes in CH_2Cl_2: (a)(ii) **1***; (a)(iv) **5***; (b)(ii) **2***; (b)(iv) **6***; (c)(ii) **3***; (c)(iv) **7***; (d)(ii) **4***; (d)(iv) **8***. The asterisk denotes the excited-state of the complexes.

Table 2 Raman bands (cm^{-1}) observed for $[(PPh_3)_2Cu(BL)\text{-}Cu(PPh_3)_2]^{2+}$ systems (CH_2Cl_2 solution)

	Mode							
Label	**1**	**2**	**3**	**4**	**5**	**6**	**7**	**8**
1		1626[a]				1629[a]		
2	1595[a]	1590[a]	1594	1591	1599	1598[a]		1602[a]
3	1555	1562	1556	1545[b]	1563	1566[a]	1557	1551
4	1514[a]	1515	1515[a]	1515[a]	1520[a]	1519	1520[a]	1523[a]
5	1491[b]			1473	1486		1483	
6	1468	1468[b]	1469	1451[b]		1470	1462	1463
7		1399[b]		1403	1390	1406	1405	1387[a]
8	1364		1363	1352[b]	1351	1352		
9	1319	1320	1329	1323[b]	1325[b]		1341	1330
10	1290	1277[b]	1291	1286[b]		1288		

[a] Preferentially enhanced with 457.9 nm excitation. [b] Preferentially enhanced with 514.5 nm excitation.

R″ = H. Only an upper bound could be determined for the excited-state lifetimes, $\tau < 50$ ns, the lifetimes were too short to be resolved reliably with the available apparatus.

The excited-state resonance Raman (ESRR) spectra of the complexes show striking differences from the ground-state spectra (Fig. 2). Studies were carried out at 448.2 nm. This wavelength is resonant with the ground-state MLCT transition, thus ensuring efficient pumping to the excited state. Coupled with the fact that it is resonant with the absorption of $dpq^{\cdot -}$,[20,28] it is therefore possible to establish an excited-state population and probe it using resonance Raman scattering with single-colour pulsed excitation.[29] Studies were carried out using varying photon fluxes up to pulse energies where the absorbed photon:molecule ratio was 3:1[30] and where no residual ground-state scattering was observed.

The spectrum of **1** shows excited-state bands at high pulse energy; no residual ground-state is present in this spectrum, as evidenced by the absence of ground-state bands at 1555, 1514,

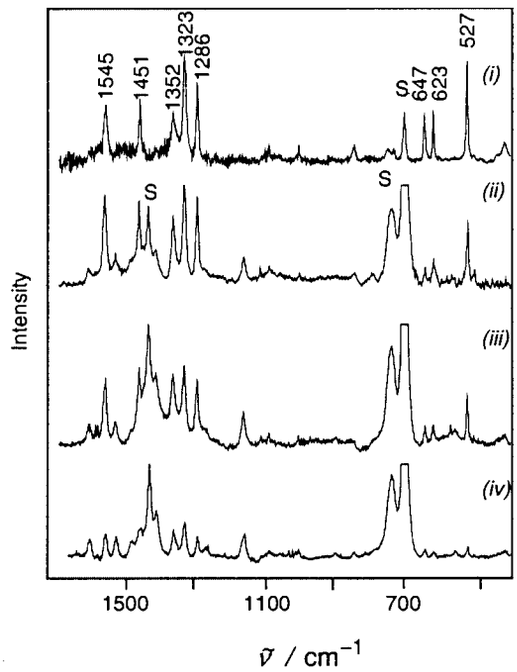

Fig. 3 Ground-state resonance Raman spectra of **4** in CH_2Cl_2 solution (10 mM concentration, 20 mW at sample): (i) λ_{exc} = 632.8 nm (60 mM solution); (ii) λ_{exc} = 514.5 nm; (iii) λ_{exc} = 488 nm; (iv) λ_{exc} = 457.9 nm.

Table 3 Raman bands (cm^{-1}) observed for $[(PPh_3)_2Cu(BL)Cu(PPh_3)_2]^{2+}$ systems with 448.2 nm pulsed excitation (CH_2Cl_2 solution)

1*	**2***	**3***	**4***	**5***	**6***	**7***	**8***
1586	1591	1588	1588	1587	1594	1588	1586
1565	1561	1551		1563	1563	1555	1565
	1514				1516		1529
1488				1484			
1467	1475	1471		1462	1467	1460	1463
	1399				1404		1383
1362			1351				
1325	1318	1328	1324	1325	1318	1337	1328
1287	1294				1278		
					1236		

1364 and 1319 cm^{-1}. The excited-state of **1**, denoted **1***, has bands at 1586, 1565, 1488 and 1467 cm^{-1}, and a weak band at 1325 cm^{-1}. This is in agreement with previous studies.[19,31] The ESRR spectrum of **5** also possesses no ground-state, as evidenced by the absence of the 1351 cm^{-1} band. The bands of **5*** are very similar in wavenumber to those of **1*** (see Table 3).

The ESRR spectra of **2** and **6** are similar to each other; no residual ground-state scattering is observed as evidenced by the absence of the 1625–1629 cm^{-1} band observed for both complexes with 457.9 nm excitation. The spectrum of **6*** shows greater enhancement of the ν_3 mode at 1563 cm^{-1} than does that of **2*** (1561 cm^{-1}).

The ESRR spectra of **3** and **7** reveal excited-state features at 1588 and about 1553 cm^{-1} (1551 cm^{-1} for **3**, and 1555 cm^{-1} for **7**), these differ from those of **1**, **2**, **5** and **6** but are the same for **3** and **7**. **3*** also shows bands at 1471 and 1328 cm^{-1} while **7*** has bands at 1460 and 1337 cm^{-1}. The spectrum of **3*** [Fig. 2(c)] has no residual ground-state, as the ground-state band at 1291 cm^{-1} is absent from the spectrum. The **7*** spectrum [Fig. 2(c)] is also entirely excited-state, as the ground-state 1520 cm^{-1} band is absent.

The ESRR spectra of **4** and **8** show a common excited-state band at 1588 cm^{-1} for **4** and 1586 cm^{-1} for **8**.

The general appearance of the ESRR spectra is similar for all of the complexes; each shows an inter-ring band at about 1320–1340 cm^{-1}, barely shifted from its position in the GSRR spectra, and some features in the 1560–1590 cm^{-1} region (Table 3). In general, the spectra appear similar for complexes which differ only by their 6′-methyl substituents. For example, the ESRR spectra of **1** and **5** show bands at similar wavenumber (1586 and 1565 cm^{-1} for **1***, 1587 and 1563 cm^{-1} for **5***). This suggests that the THEXI-state is similar in both cases and this would be consistent with occupation of a ligand π^* MO that is strongly polarised to the quinoxaline ring system. The radical anion spectrum of dpq has been measured spectroelectrochemically for **1** and related rhenium(I) complexes.[28] The spectrum of $[Re(CO)_3Cl(dpq)]^-$ shows strong bands at 1586 and 1565 cm^{-1}, coincident with those observed for **1***. However, these differ significantly from the spectrum observed for $[Re(CO)_3Cl(dpq)Re(CO)_3Cl]^-$; this shows bands at 1604, 1562 and 1327 cm^{-1}, with a stronger enhancement of the low wavenumber mode.[32] This finding was rationalised as being due to polarisation of charge to the pyridyl rings in the binuclear rhenium(I) complex, caused by the strong charge-stabilising effect of the two Re(I) centres. The $[Cu(PPh_3)_2]^+$ moiety is well known to be less stabilising of charge and is unable to distort the charge localisation in the manner observed for the binuclear rhenium(I) complexes.

The radical anion feature observed at about 1580 cm^{-1} appears to be a quinoxaline-based mode from the fact that it shifts with quinoxaline substitution, but not 6-methyl group substitution at the pyridyl. A shift to higher wavenumber upon reduction of a ligand is by no means unusual.[33] We propose that the 1570–1590 cm^{-1} band is the ν_3 mode. This would correspond to shifts of about 20–30 cm^{-1}, such shifts have been reported in the radical anion spectra of other polypyridyl ligands. The very small shifts in the wavenumber for the inter-ring stretch on going from the ground-state to the excited-state are indicative of small bond changes at the C2–C2″ or C3–C2′ linkages upon formation of the radical anion in the MLCT excited-state. This is consistent with previous computational and experimental studies.[18]

This interpretation of the excited-state Raman data is consistent with electron spin resonance experiments on $[\{Ru(bpy)_2\}_2(\mu\text{-dpq})]^{4+}$ that show the unpaired electron localised to the quinoxaline ring of the dpq bridging ligand.[19] That the excited-state electron distribution is independent of the nature of the substituent at the pyridyl ring may be the result of a geometry change following photoexcitation.

The GSRR data provide an insight into the state(s) initially populated by MLCT excitation at differing wavelengths. These data suggest that with λ_{exc} = 457.9 nm the transition populates a π^* MO on the ligand that has significant pyridyl character, as the λ_{exc} is tuned to the red a lower energy transition becomes resonant which terminates across the quinoxaline ring. One surprising result of this is that the GSRR spectra at long λ_{exc} show strong enhancement of the inter-ring stretch mode (ν_9), yet the ESRR spectra shows a band unshifted from the corresponding ground-state ν_9 in all of the complexes studied. The GSRR data suggest significant distortion of the inter-ring bond, consistent with the population of a π^* MO with amplitude at the C2–C2″ and C3–C2′ linkages (Fig. 1), yet the ESRR data suggest little change in bond order across those linkages. There are a number of possible reasons for this observation:
(1) The relative enhancement of different modes, *e.g.* ν_9 *versus* ν_3, may oscillate with excitation wavelength under certain conditions. Primary among these is a low damping factor (Γ) for the resonant transition. It is possible that the apparent strong enhancement of ν_9 is a consequence of the oscillation rather than indicating a large Δ.[34,35] This hypothesis may be tested by measuring the spectrum under pre-resonance conditions,[8] as under such conditions Γ is large.[35] The spectrum of **4** measured with 632.8 nm excitation shows the enhancement of 3 modes [Fig. 3(i)] in the 1000–1600 cm^{-1} region. The strongly enhanced modes are the same as those enhanced at 514.5 nm excitation,

suggesting that the Γ for the transition is large. This means the enhanced ν_9 mode indicates a significant Δ along that normal mode.

(2) The FC-state probed in the GSRR spectra with 514.5 nm excitation has a different electronic configuration from the THEXI-state. Previous semi-empirical calculations on the ligand dpq in the conformation in which it is found in **1** showed the presence of two low-lying UMOs which differed significantly in their wavefunction amplitude at the inter-ring linkages. If the MLCT transition resonant in the GSRR spectra terminated on the π^* ligand MO, resulting in a significant inter-ring bonding change, then the ν_9 mode would be enhanced, but if the THEXI-state had the excited electron in the MO with a non-bonded character across the inter-ring then there would be very little perturbation in the wavenumber of the ν_9 mode.

(3) The resonance enhancement from the THEXI-state results in the enhancement of a vibration associated with one of the inter-ring bonds that has been relatively unchanged by population of the MLCT-state. This may occur because the MLCT excited-state renders the molecule asymmetric from C_2 symmetry because only one copper(I) site is oxidised. As a result of this one of the sides of the ligand is flattened out. X-Ray crystallographic data suggest the dihedral angle for a copper(II) dpq complex is *ca.* 25°,[36] whereas that for **1** is *ca.* 32°.[20] In order to understand these potential changes, a series of calculations were performed.

For these calculations, three approximations to the reported crystal structure of **1** were made. The Cu moieties were omitted due to a limitation of confidence with the PM3 method beyond the first row elements. In a study of ruthenium(II) complexes, calculations of the electron localisation on the bipyridyl ligands was modelled with substituted pyridine moieties. The validity of this simplification was that the metal moiety interacts with the ligand predominately through the σ-bonding system, whereas the photophysics are dominated by the π-system of the ligand.[37] This argument should be more valid given that the Cu(I) moiety has a smaller influence on the electronic nature of the ligand than a Ru(II) moiety.[38]

Three structural forms of dpq were studied: 0/30-dpq, 15/30-dpq and 30/30-dpq. The numbers correspond to constraints placed on the dihedral angles between each of the pyridyl rings and the quinoxaline ring system, as shown in Fig. 1 (defined as the dihedral angle between N1″–C2″–C2–N1). The 30/30-dpq form represents constraints associated with coordination of two $[Cu(PPh_3)_2]^+$ moieties. The 0/30-dpq is a limiting representative form of the constraints placed upon the dihedral angle by coordination of a Cu(II) and a Cu(I) moiety, respectively. The large change in dihedral angle was chosen to both bracket the limiting forms of dpq and to aid in visualisation. The 15/30-dpq form was selected as another data point in the quantum chemical experiment.

To model the electronic form of dpq in the excited-state, the dianion form of dpq was studied: dpq^{2-}. Calculations on the radical anion were avoided due to problems associated with open shell configurations.[39] Although the dianion represents the addition of two electrons to the LUMO, this configuration brackets the actual configuration. In regard to the present study, the presence or absence of spectral shifts are the primary concern and the calculations were not undertaken to provide a detailed quantitative understanding of the spectral changes observed.

Geometry optimisation and single point energy calculations were carried out to determine the inter-ring bond distance and the form of the molecular orbitals on 0/30-dpq, 15/30-dpq, 30/30-dpq and the dianion forms, respectively, 0/30-dpq^{2-}, 15/30-dpq^{2-}, 30/30-dpq^{2-}. The 0/30-dpq and 15/30-dpq forms of the neutral ligand were studied to assess any inter-ring bond length changes independent from the addition of 2 electrons. The inter-ring bond lengths (r) for the 3 conformations of dpq and dpq^{2-} are shown in Fig. 4.

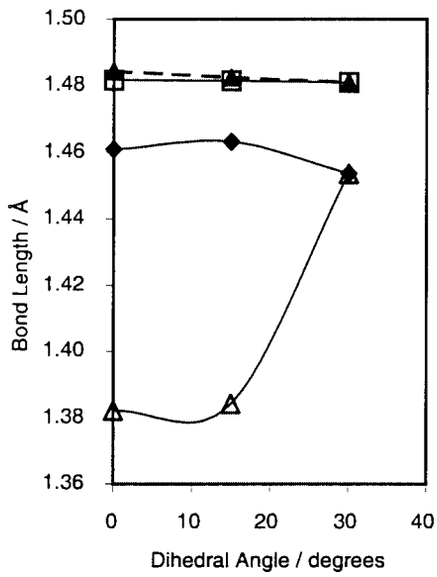

Fig. 4 Plot of the variation in bond lengths (r) for the C2–C2″ and C3–C2′ linkages (Fig. 1) *versus* dihedral angle (as defined by N1″–C2″–C2–N1) for dpq and its dianion. ▲ r(C2–C2″) dpq; □ r(C3–C2′) dpq; △ r(C2–C2″) dpq^{2-}; ◆ r(C3–C2′) dpq^{2-}.

There are 2 striking results from these calculations: (a) The inter-ring bond length r(C2–C2″) is significantly shortened by the flattening of the dihedral angle when electron density is added to the LUMO. (b) The other side of the dpq has little change in inter-ring bond length r(C3–C2′).

It should be noted that the shortening of r(C2–C2″) is not observed for the neutral dpq with variation in dihedral angle (Fig. 4).

For the GSRR experiment, enhancement of the inter-ring results from the changes in the bond length associated with the FC-state, *i.e.* dihedral angle 30° (Fig. 4). However the ESRR variant will enhance modes associated with its resonance transition; that is for the ligand in its THEXI conformation. This has r(C2–C2″) significantly shortened and r(C3–C2′) slightly lengthened from the FC-state. The enhancement pattern will result from geometry changes for the resonant radical anion transition, which is $\pi \longrightarrow \pi^*$ in nature. If this transition results in a change in r(C3–C2′) then the ν_9 mode would be enhanced; however the wavenumber of the ν_9 mode would be similar to that for the ground-state because the bond length is almost the same as in dpq.

(4) The ESRR experiment may be probing a different mode from that of the GSRR spectroscopy and this new mode is coincident with the ν_9 vibration. This seems unlikely to occur for all of the complexes observed.

The most likely explanation for the observed spectral changes, notably the enhancement of the ν_9 mode in the GSRR spectra and its appearance in the ESRR spectra at the same wavenumber, are given by options (2) and (3). The observation of strong enhancement of low wavenumber out-of-plane modes (*e.g.* 527 cm^{-1}, Fig. 3) indicates a strong distortion of the ligand upon photoexcitation. This is supportive of option (3).

Conclusions

Analysis of the resonance Raman intensities in the ground-state has provided a qualitative description of the geometry changes following photoexcitation. The wavenumbers of the bands observed in the excited-state have provided similar information for the THEXI-state structure. The GSRR spectra reveal the presence of two MLCT chromophores in the visible region. The higher energy absorbing chromophore has an acceptor orbital with significant polarisation toward the pyridyl rings, the lower

energy transition appears more polarised to the quinoxaline. The THEXI-state appears to have an electronic configuration in which the acceptor orbital is predominantly quinoxaline in nature. Quantum chemical calculations suggest the inter-ring bonds connecting the pyridyl to quinoxaline rings are shortened to differing extents, depending on the flattening of the ligand. This offers an explanation for the observation of an unshifted ν_9 mode in the ESRR spectra.

Acknowledgements

Support from the New Zealand Lottery Commission and the University of Otago Research Committee for the purchase of the Raman spectrometer is gratefully acknowledged. M. R. W. thanks the John Edmond postgraduate scholarship and the Shirtcliffe fellowship for support for Ph.D. research and The Royal Society of New Zealand for the award of a Beginning Scientist Award. A. F. thanks the Alliance Group Postgraduate Scholarship award.

References

1 M. K. Nazeeruddin, A. Kay, I. Rodicio, R. Humphrey-Baker, E. Mueller, P. Liska, N. Vlachopoulos and M. Gratzel, *J. Am. Chem. Soc.*, 1993, **115**, 6382; K. Kalyanasundaram and M. Gratzel, *Coord. Chem. Rev.*, 1998, **177**, 347; J. E. Moser, P. Bonnote and M. Gratzel, *Coord. Chem. Rev.*, 1998, **177**, 245; C. A. Bignozzi, J. R. Schoonover and F. Scandola, *Prog. Inorg. Chem.*, 1997, **44**, 1.

2 V. Balzani, M. Gomez-Lopez and J. F. Stoddart, *Acc. Chem. Res.*, 1998, **31**, 405; M. Venturi, S. Serroni, A. Juris, S. Campagna and V. Balzani, *Top. Curr. Chem.*, 1998, **197**, 193; V. Balzani, S. Campagna, G. Denti, A. Juris, S. Serroni and M. Venturi, *Acc. Chem. Res.*, 1998, **31**, 26; R. Ziessel, M. Hissler, A. El-Ghayoury and A. Harriman, *Coord. Chem. Rev.*, 1998, **180**, 1251; R. Ziessel and A. Harriman, *Coord. Chem. Rev.*, 1998, **171**, 331; F. Scandola, R. Argazzi, C. A. Bignozzi, C. Chiorboli, M. T. Indelli and M. A. Rampi, in *Supramolecular Chemistry*, ed. V. Balzani and L. DeCola, Kluwer Academic Publishers, Netherlands, 1992, p. 235; L. De Cola and P. Belser, *Coord. Chem. Rev.*, 1998, **177**, 301; M. D. Ward, C. M. White, F. Barigelletti, N. Armaroli, G. Calogero and L. Flamigni, *Coord. Chem. Rev.*, 1998, **171**, 481.

3 M. K. Eggleston, D. R. McMillin, K. S. Koenig and A. J. Pallenberg, *Inorg. Chem.*, 1997, **36**, 172; M. T. Miller, P. K. Gantzel and T. B. Karpishin, *J. Am. Chem. Soc.*, 1999, **121**, 4292; M. Ruthkosky, C. A. Kelly, M. C. Zaros and G. J. Meyer, *J. Am. Chem. Soc.*, 1997, **119**, 12004.

4 J. H. Elias and R. S. Drago, *Inorg. Chem.*, 1972, **11**, 415; R. W Callahan, G. M. Brown and T. J Meyer, *Inorg. Chem.*, 1975, **14**, 1443; C. Creutz, *Prog. Inorg. Chem.*, 1983, **30**, 1.

5 S.-Y. Lee and E. J. Heller, *J. Chem. Phys.*, 1979, **71**, 4777; D. J. Tannor and E. J. Heller, *J. Chem. Phys.*, 1982, **77**, 202; E. J. Heller, R. L. Sundberg and D. J. Tannor, *J. Phys. Chem.*, 1982, **86**, 1822.

6 A. B. Myers, *Excited Electronic State Properties from Ground-State Resonance Raman Intensities*, in *Laser Techniques in Chemistry*, ed. A. B. Myers and T. R. Rizzo, Wiley, New York, 1995.

7 M. Tsuboi and A. Y. Hirakawa, *Science*, 1975, **188**, 359.

8 S. K. Doorn and J. T. Hupp, *J. Am. Chem. Soc.*, 1989, **111**, 1142; V. Petrov, J. T. Hupp, C. Mottley and L. C. Mann, *J. Am. Chem. Soc.*, 1994, **116**, 2171.

9 A. W. Adamson, *J. Chem. Educ.*, 1983, **60**, 797.

10 H. A. Goodwin and F. Lions, *J. Am. Chem. Soc.*, 1959, **81**, 6415.

11 V. W.-W. Yam and K. K.-W. Lo, *J. Chem. Soc.*, *Dalton Trans.*, 1995, 499.

12 D. B. Shriver and B. R. Dunn, *Appl. Spectrosc.*, 1974, **28**, 319.

13 R. P. Van Duyne and K. D. Parks, *Chem. Phys. Lett.*, 1980, **76**, 196; C. A. Grant and J. L. Hardwick, *J. Chem. Educ.*, 1997, **74**, 318.

14 The ASTM subcommittee on Raman spectroscopy has adopted eight materials as Raman shift standards (ASTM E 1840). The band wavenumbers for these standards are available at http://chemistry.ohio-state.edu/~rmccreer/shift.html. Methods for correcting Raman spectra are given at http://chemistry.ohio-state.edu/~rmccreer/intensty/intensty.html. The Raman spectrum of cyclohexane obtained from our instrument was compared to literature values and corrected where appropriate. This correction factor was applied to the GSRR spectrum of **4** at 632.8 nm excitation.

15 PC SPARTAN Plus version 1.5, Wavefunction, Inc., 18401 Von Karman Ave., Suite 370, Irvine, CA 92612, 1998.

16 M. R. Waterland, K. C. Gordon and A. K. Burrel, manuscript in preparation.

17 D. J. Casadonte, Jr. and D. R. McMillin, *J. Am. Chem. Soc.*, 1987, **109**, 331.

18 K. C. Gordon, A. H. R. Al-Obaidi, P. M. Jayaweera, J. J. McGarvey, J. F. Malone and S. E. J. Bell, *J. Chem. Soc.*, *Dalton Trans.*, 1996, 1591.

19 F. R. Dollish, W. G. Fateley and F. F. Bentley, *Characteristic Raman Frequencies of Organic Compounds*, Wiley, New York, 1974.

20 J. B. Cooper, D. B. MacQueen, J. D. Petersen and D. W. Wertz, *Inorg. Chem.*, 1990, **29**, 3701.

21 J. R. Schoonover, P. Chen, W. D. Bates, R. B. Dyer and T. J. Meyer, *Inorg. Chem.*, 1994, **33**, 793; R. A. McNichol, J. J. McGarvey, A. H. R. Al-Obaidi, S. E. J. Bell, P. M. Jayaweera and C. G. Coates, *J. Phys. Chem.*, 1995, **99**, 12268.

22 D. P. Strommen, P. K. Mallick, G. D. Danzer, R. S. Lumpkin and J. R. Kincaid, *J. Phys. Chem.*, 1990, **94**, 1357; P. K. Mallick, G. D. Danzer, D. P. Strommen and J. R. Kincaid, *J. Phys. Chem.*, 1988, **92**, 5628.

23 T. J. Durnick and S. C. Wait, Jr. *J. Mol. Spectrosc.*, 1972, **42**, 211.

24 S. M. Scott, A. K. Burrell, P. A. Cocks and K. C. Gordon, *J. Chem. Soc.*, *Dalton Trans.*, 1998, 3679; J. Sherborne, S. M. Scott and K. C. Gordon, *Inorg. Chim. Acta*, 1997, **260**, 199; J. Sherborne and K. C. Gordon, *Asian J. Spectrosc.*, 1998, **2**, 137.

25 G. D. Danzer, J. A. Golus and J. R. Kincaid, *J. Am. Chem. Soc.*, 1993, **115**, 8643.

26 K. M. Omberg, G. D. Smith, D. A. Kavaliunas, P. Chen, J. A. Treadway, J. R. Schoonover, R. A. Palmer and T. J. Meyer, *Inorg. Chem.*, 1999, **38**, 951; P. Chen, K. M. Omberg, D. A. Kavaliunas, J. A. Treadway, R. A. Palmer and T. J. Meyer, *Inorg. Chem.*, 1997, **36**, 954.

27 D. P. Strommen, *J. Chem. Educ.*, 1992, **69**, 803; R. J. H. Clark and T. J. Dines, *Angew. Chem.*, *Int. Ed. Engl.*, 1986, **25**, 131.

28 M. R. Waterland, T. J. Simpson, K. C. Gordon and A. K. Burrell, *J. Chem. Soc.*, *Dalton Trans.*, 1998, 185.

29 P. G. Bradley, N. Kress, B. A. Hornberger, R. F. Dallinger and W. H. Woodruff, *J. Am. Chem. Soc.*, 1981, **103**, 7441; P. A. Mabrouk and M. S. Wrighton, *Inorg. Chem.*, 1986, **25**, 526; K. C. Gordon and J. J. McGarvey, *Chem. Phys. Lett.*, 1989, **162**, 117.

30 At 2 mJ pulse^{-1} with a spot size of 300 μm, sample penetration of *2 mm and sample concentration of* 1×10^{-2} mol L^{-1} the number *of molecules in the irradiated volume is less than* 10^{15}, the number of photons per pulse is 4.5×10^{15}.

31 K. C. Gordon and J. J. McGarvey, *Chem. Phys. Lett.*, 1990, **173**, 443.

32 T. J. Simpson and K. C. Gordon, *Inorg. Chem.*, 1995, **34**, 6323.

33 G. Buntinx, O. Poizat and N. Leygue, *J. Phys. Chem.*, 1995, **99**, 2343.

34 J. I. Zink and K.-S. K. Shin, *Adv. Photochem.*, 1991, **16**, 119.

35 J. I. Zink and K.-S. K. Shin, *Inorg. Chem.*, 1989, **28**, 4358.

36 K. V. Goodwin, W. T. Pennington and J. D. Petersen, *Acta Crystallogr.*, *Sect. C*, 1990, **46**, 898.

37 N. H. Damrauer, B. T. Weldon and J. K. McCusker, *J. Phys. Chem. A*, 1998, **102**, 3382.

38 S. M. Scott, A. K. Burrell, P. A. Cocks and K. C. Gordon, *J. Chem. Soc.*, *Dalton Trans.*, 1998, 3679; S. M. Scott, A. K. Burrell and K. C. Gordon, *J. Chem. Soc.*, *Dalton Trans.*, 1998, 2873; S. M. Scott, K. C. Gordon and A. K. Burrell, *Inorg. Chem.*, 1996, **35**, 2452.

39 Preliminary calculations on the radical anion reveal high values for the spin expectation parameter; $\langle S^2 \rangle = 1.5201$ (0/30-dpq$^{\bullet -}$), 1.3936 (15/30-dpq$^{\bullet -}$) and 0.8531 (30/30-dpq$^{\bullet -}$). See ref. 38.

Paper a909121a